*J. Plasma Physics* (2011), *vol.* 77, *part* 3, *pp.* 345–356.  
doi:10.1017/S0022377810000607

# Numerical analysis of double layers in the downward current region of the aurora

SANQIU LIU[1] and JINGJING LIAO[2]

[1]Department of Physics, Nanchang University, Nanchang 330047, P.R. China
[2]Department of Information and Engineering, Jiangxi University of Science and Technology, Ganzhou 341000, P.R. China
(sqlgroup@ncu.edu.cn)

(Received 3 April 2010; revised 6 May 2010; accepted 6 September 2010, first published online 8 October 2010)

**Abstract.** On the basis of two magneto-fluid model for two time-scales, the evolution of double layer in the downward current region of the aurora is numerically simulated under the non-static limit case. The results show that localized drop in density owing to collapsed high-frequency field can lead to the formation of double layer. The amplitude of the double layer is the order of the electron temperature, and the ramp potential is up to 36 V localized to tens of Debye lengths, which is around 100–200 m. These are consistent with the measurements in both the ramp potential and thickness by the Fast Auroral SnapshoT satellite in the downward current region of the aurora.

## 1. Introduction

Since Alfvén et al. [1] has suggested the current disruption theory for solar flare, the subject of double layer (DL) has attracted great attention. Many space observations [2–4], laboratory experiments [5–7], numerical simulations [8–9] and theoretical studies [10–11] about double layers have been undertaken. It turns out that double layer is a local structure in the plasma, which is capable of sustaining high potential drops [12]. Typically, these are quoted as having a width of tens of Debye lengths, $\lambda_D$ (the correlation length for potential fluctuations in a plasma). The amplitude of space double layers seems to be in the range of 1–100 eV.

Double layers have been invoked in auroral plasmas [13] to explain the downward acceleration of kilovolt electrons that collide with the upper atmosphere and produce the visible aurora. These have been observed by the Fast Auroral SnapshoT (FAST) satellite in the downward current region of the auroral ionosphere [14–15]. These observations reveal that small double layers, their amplitude being of the order of the electron temperature, can provide a sufficient field-aligned potential change to accelerate electrons. The ramp potential of the double layer is in range of 14–40 V and the thickness of the structure is between 100 and 200 m, roughly tens of $\lambda_D$. The electron temperature is $T_e \sim 9$ eV, and the density, $n_e \sim 20$ cm$^{-3}$.

In theoretical studies, much effort has been directed toward explaining possible mechanisms of formation for electrostatic double layers. In short, maintenance of double layer is possible only if there exists multiple plasma sources or a current drive [16]. In general, the current in an electron stream is virtually constant because the temporal electron transients and pressure are ignored in the fluid model. Any disturbance resulting in localized density depressions would develop and generate

current-driven instabilities, leading to the formation of double–double layers. As the magnetosphere–ionosphere current system at auroral latitudes involves processes on a vast spatial scale compared to the tens of Debye lengths of the observed double layers, it is more likely that initially the plasma carries a current that drives the formation of a double layer at the site of some inhomogeneity, with the resulting potential jump being an effect of the double layer [17]. Therefore, there exists a current drive to maintain the double layer in the downward current region of the aurora.

In 1979, Raadu et al. [18] showed that a local evacuation instability in a current-driven plasma can be the possible mechanism for double layer formation. Another mechanism examined by Carlqvist [19] in 1980 was the anomalous resistivity caused by two-stream or ion acoustic instabilities. But effects of high-frequency oscillations on low frequency and slow motion have been never considered. It is well known that two magneto-fluid systems will be controlled by modulational instability in consideration of the oscillations [20]. A traveling wave solution in one dimension of the double layer by solving the Zakharov equations by making two time-scale approximations for two-fluid equations is obtained by Li [16]. It is shown that double layer is a nonlinear entity in this case: soliton and wave-packet shock. However, the analytical solutions for two- or three-dimension double layers have not been found because of the complexity of the equations. To gain a deeper and more intuitive picture of the double layer formation, computer simulations in two or three dimensions are necessary. Numerous authors have investigated many problems, such as density caviton, by solving numerically the Zakharov equations in two and three dimensions [21–23]. However, in their simulation, a Cartesian coordinate system is used and the problem for double layers is not considered. The present paper is devoted to the double layer study in the downward current region of the aurora that is numerically controlled by modulational instability on the basis of two magneto-fluid models for two time-scales under the non-static limit case. Considering that the particle stream and radiation flux in the downward current region of the aurora appear to be axially symmetrical, it is important to investigate the problem in cylindrical coordinates with axisymmetry. The evolution of the double layer, density cavity and collapsed electric field takes place. At the same time, the ramp potential and thickness of the double layer in the downward current regions of the aurora, which are similar to the measurements [14–15] in both the ramp potential and thickness by the FAST satellite, are obtained.

This paper is organized as follows: In Sec. 2, we introduce the nonlinear coupling equations of low-frequency potential, high-frequency field and density disturbance on the basis of two magneto-fluid models for two time-scales that govern the mechanism of double layer formation in the downward current region of the aurora. Section 3 gives the results of numerical calculation. Finally, the conclusion and discussion are presented in Sec. 4.

## 2. Nonlinear coupling equations

The motion of plasmas satisfies the two-fluid equations in the situation of high-frequency oscillations, as follows:

$$\frac{\partial n_e}{\partial t} + \nabla \cdot (n_e \mathbf{v}_e) = 0, \tag{2.1}$$

https://doi.org/10.1017/S0022377810000607 Published online by Cambridge University Press

$$\frac{\partial n_i}{\partial t} + \nabla \cdot (n_i \mathbf{v}_i) = 0, \tag{2.2}$$

$$\frac{\partial \mathbf{v}_e}{\partial t} + (\mathbf{v}_e \cdot \nabla)\mathbf{v}_e = \frac{e}{m_e}\left(\mathbf{E} + \frac{1}{c}\mathbf{v}_e \times \mathbf{B}\right) - \frac{\gamma_e T_e}{m_e n_e}\nabla n_e, \tag{2.3}$$

$$\frac{\partial \mathbf{v}_i}{\partial t} + (\mathbf{v}_i \cdot \nabla)\mathbf{v}_i = \frac{e_i}{m_i}\left(\mathbf{E} + \frac{1}{c}\mathbf{v}_i \times \mathbf{B}\right) - \frac{\gamma_i T_i}{m_i n_i}\nabla n_i, \tag{2.4}$$

$$\nabla \times \mathbf{E} = -\frac{1}{c}\frac{\partial \mathbf{B}}{\partial t}, \tag{2.5}$$

$$\nabla \times \mathbf{B} = \frac{1}{c}\frac{\partial \mathbf{E}}{\partial t} + \frac{4\pi}{c}(e n_e \mathbf{v}_e + e_i n_i \mathbf{v}_i), \tag{2.6}$$

where subscripts $e$ and $i$ represent electrons and ions, respectively, $\gamma_e$ and $\gamma_i$ are the specific heat ratios for electrons and ions, respectively, and other symbols have common implications.

On account of a great difference for electron and ion oscillation frequency in the cosmic plasma, we can distinguish two time-scales: slow ion time-scale, $t_s \sim \omega_{pi}^{-1}$, and fast electron time-scale, $t_f \sim \omega_{pe}^{-1}$, where $\omega_{pe} = \sqrt{\frac{4\pi e^2 n_e}{m_e}}$ and $\omega_{pi} = \sqrt{\frac{4\pi e_i^2 n_i}{m_i}}$. As a result of interaction between electromagnetic field and particles in plasma, there are two time-scale components for the density and velocity of a moving electron, but only slow time-scale components are present for the ion due to its large inertia. As far as electric and magnetic fields are concerned, we can assume that only magnetic field has the fast time-scale component, and the electric field involves two components. As we are interested in instability that is developed in the background of slow time-scale, in a natural way we can suggest that the average value of fast time-scale over slow time-scale vanishes. Hence, we can consider parameters of fast time-scale as turbulent ones: their characteristic time of phase shift, $\tau \sim t_f \ll t_s$, then the condition of random phase approximation is fulfilled. In addition, on a slow time-scale, quasi-neutrality condition is valid. Therefore, we obtain the following Zakharov equations and the low-frequency potential that result in separating the charges [16, 20, 22]:

$$2i\omega_{pe}\frac{\partial \mathbf{E}(\mathbf{r}, t)}{\partial t} + c^2 \nabla \times \nabla \times \mathbf{E}(\mathbf{r}, t) - \gamma_e v_{Te}^2 \nabla(\nabla \cdot \mathbf{E}(\mathbf{r}, t)) + \frac{\delta n}{n_0}\omega_{pe}^2 \mathbf{E}(\mathbf{r}, t) = 0, \tag{2.7}$$

$$\left(\frac{\partial^2}{\partial t^2} - c_s^2 \nabla^2\right)\frac{\delta n}{n_0} = \nabla^2\left(\frac{|\mathbf{E}(\mathbf{r}, t)|^2}{16\pi n_0 m_i}\right), \tag{2.8}$$

$$|e|\,\phi = \gamma_e T_e \frac{\delta n}{n_0} + \frac{|\mathbf{E}(\mathbf{r}, t)|^2}{16\pi n_0}, \tag{2.9}$$

where $c_s = \sqrt{\frac{\gamma_e T_e + \gamma_i T_i}{m_i + m_e}}$ is the sound velocity, $n_0$ is the undisturbed particle density, $|\delta n| \ll n_0$ is the disturbed particle density and $\phi$ is the low-frequency electric potential that comes from the slow time-scale component of electric field, $\mathbf{E}_s$, i.e. $\mathbf{E}_s = -\nabla\phi$. $\mathbf{E}(\mathbf{r}, t)$ is the envelope of the high-frequency electric field $\mathbf{E}_f$. Equations (2.7) and (2.8) are well known identities [20, 22]. For transverse plasmons near the plasma frequency $\omega_{pe}$, $\mathbf{E}_f$ can be expressed as $\mathbf{E}_f = \frac{1}{2}[\mathbf{E}(\mathbf{r}, t)e^{i\omega_{pe}t} + c.c.]$, where the envelope

https://doi.org/10.1017/S0022377810000607 Published online by Cambridge University Press

field $\mathbf{E}(\mathbf{r},t)$ varies slowly compared with $\omega_{pe}$ [24]. Here *c.c.* denotes the complex conjugate of the first term.

Through the substitutions,

$$\hat{\mathbf{r}} = \frac{2}{3}\frac{\omega_{pe}}{c_s}\mu\mathbf{r},\ \tau = \frac{2}{3}\mu\omega_{pe}t,\ \hat{n} = \frac{3}{4\mu}\frac{\delta n}{n_0},\ \hat{\phi} = \frac{|e|\,\phi}{T_e},$$

$$\hat{\mathbf{E}}(\hat{\mathbf{r}},\tau) = \frac{\sqrt{3}\mathbf{E}(\mathbf{r},\ t)}{8[\pi n_0\mu(\gamma_e T_e + T_i)]^{1/2}},\ \mu = \frac{m_e}{m_i},\ \alpha = \frac{c^2}{3v_{Te}^2}.$$

Equations (2.7)–(2.9) can be written as follows [16, 20, 22]:

$$i\frac{\partial}{\partial\tau}\mathbf{E}(\mathbf{r},\tau) + \alpha\nabla\times\nabla\times\mathbf{E}(\mathbf{r},\tau) - \nabla(\nabla\cdot\mathbf{E}(\mathbf{r},\tau)) + n\mathbf{E}(\mathbf{r},\tau) = 0, \tag{2.10}$$

$$\left(\frac{\partial^2}{\partial\tau^2} - \nabla^2\right)n = \nabla^2\left|\mathbf{E}(\mathbf{r},\tau)\right|^2, \tag{2.11}$$

$$\phi = \frac{4\gamma_e\mu n}{3} + \frac{16\mu\left|\mathbf{E}(\mathbf{r},\tau)\right|^2}{3}. \tag{2.12}$$

(The hat matrix is omitted in the above quantities.) Equations (2.10)–(2.12) are the nonlinear coupling equations of high-frequency field, density disturbance and low-frequency potential under the non-static limit case. The key mechanism of the double layer formation in the downward current region of the aurora is governed by the above equations. The term on the right-hand side of (2.11) is from the ponderomotive force of high-frequency field. Under the static limit case, the first term on the left-hand side of (2.11) is less than the second term: $\frac{\partial^2}{\partial\tau^2} \ll \nabla^2$, that is $|\frac{d\mathbf{r}}{dt}|_{\text{collapse}} \ll c_s$ in dimensional unit. Therefore, the first term can be overlooked, and the coupling equations under the static limit can be derived [22]. The parameter of turbulence is

$$\hat{W} = \frac{\langle(\mathbf{E}_f)^2\rangle}{4\pi n_0 T_e} = \frac{|\mathbf{E}(\mathbf{r},\ t)|^2}{8\pi n_0 T_e} = \frac{8}{3}\mu|\hat{\mathbf{E}}(\hat{\mathbf{r}},\ \tau)|^2. \tag{2.13}$$

## 3. Numerical calculation

In order to investigate more deeply and intuitively the double layer formation in the downward current region of the aurora, (2.10)–(2.12) are numerically calculated in cylindrical coordinate system with axisymmetry. The variables are only dependent on $r$ and $z$, and all partial derivative terms to $\varphi$ vanish. Much of the electromagnetic emission, such as auroral kilometric radiation (AKR), which originated in the auroral zones, has been observed. Perhaps the electrostatic Langmuir emission exists, but its strength can't be estimated. Therefore, we only consider the electromagnetic interaction with plasma and not the electrostatic Langmuir turbulence. In this case, (2.10)–(2.12) can be converted into

$$i\frac{\partial E_r}{\partial\tau} - \alpha\left(\frac{\partial^2 E_r}{\partial r^2} + \frac{\partial^2 E_r}{\partial z^2} + \frac{1}{r}\frac{\partial E_r}{\partial r} - \frac{E_r}{r^2}\right) + nE_r = 0, \tag{3.1}$$

$$i\frac{\partial E_\varphi}{\partial\tau} - \alpha\left(\frac{\partial^2 E_\varphi}{\partial r^2} + \frac{\partial^2 E_\varphi}{\partial z^2} + \frac{1}{r}\frac{\partial E_\varphi}{\partial r} - \frac{E_\varphi}{r^2}\right) + nE_\varphi = 0, \tag{3.2}$$

https://doi.org/10.1017/S0022377810000607 Published online by Cambridge University Press

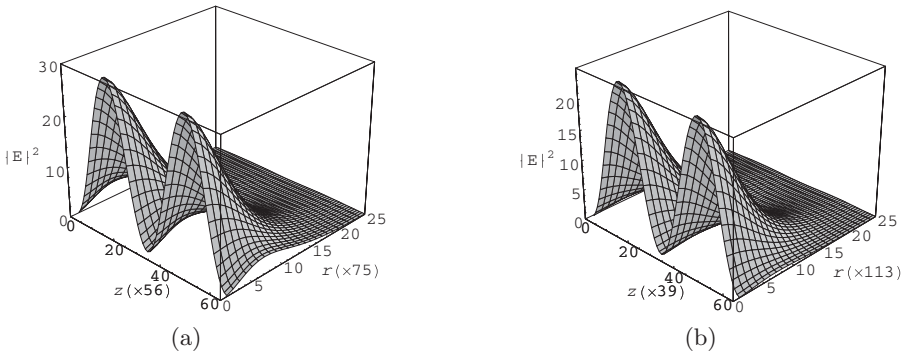


**Figure 1.** The distribution of initial electric field: (a) $\tau = 0, |\mathbf{E}|^2_{\max} = 30$, (b) $\tau = 0, |\mathbf{E}|^2_{\max} = 25$.

$$i\frac{\partial E_z}{\partial \tau} - \alpha\left(\frac{\partial^2 E_z}{\partial r^2} + \frac{\partial^2 E_z}{\partial z^2} + \frac{1}{r}\frac{\partial E_z}{\partial r}\right) + nE_z = 0, \tag{3.3}$$

$$\left(\frac{\partial^2}{\partial \tau^2} - \frac{\partial^2}{\partial r^2} - \frac{1}{r}\frac{\partial}{\partial r} - \frac{\partial^2}{\partial z^2}\right)n = \left(\frac{\partial^2}{\partial r^2} + \frac{1}{r}\frac{\partial}{\partial r} + \frac{\partial^2}{\partial z^2}\right)\left(E_r^2 + E_\varphi^2 + E_z^2\right), \tag{3.4}$$

$$\phi = \frac{4\gamma_e \mu n}{3} + \frac{16\mu(E_r^2 + E_\varphi^2 + E_z^2)}{3}. \tag{3.5}$$

We use time forward-difference and space central-difference method (FTCS) as the numerical method to solve the coupling equations in two dimensions with three components under the condition of a finite amplitude transverse wave. Meanwhile, the periodic boundary condition in the $z$-axis is used. In the $r$-direction, a natural boundary condition is considered in the calculation, i.e. the field tends to zero when $r \to \infty$. The initial field, suitable for the condition of transverse wave, i.e. $\nabla \cdot \mathbf{E}(\mathbf{r}, \tau = 0) = 0$, is chosen as

$$\begin{aligned}\mathbf{E}(\mathbf{r}, \tau = 0) &= E_0 \sin\left(\frac{2\pi z}{z_0}\right) \sec h\left(\frac{r}{r_0}\right)\mathbf{e}_r + E_0 \sin\left(\frac{2\pi z}{z_0}\right) \sec h\left(\frac{r}{r_0}\right)\mathbf{e}_\varphi \\ &\quad - E_0\left(\frac{z_0}{2\pi r_0}\right)\cos\left(\frac{2\pi z}{z_0}\right)\tanh\left(\frac{r}{r_0}\right)\sec h\left(\frac{r}{r_0}\right)\mathbf{e}_z,\end{aligned} \tag{3.6}$$

where $z_0$ and $r_0$ are the period and width of the transverse wave, respectively. The spatial range of the numerical simulation is chosen as $\Delta z = z_0$ and $\Delta r = 8r_0$. Figure 1 describes the distribution of the initial electric field. The evolution of the solution for (3.1)–(3.5) with (3.6) as the initial condition is given in Figs 2–7. The collapse development and level contours of electric potential $\phi$ are shown in Figs 2 and 5, the collapse development of density disturbance $n$ is shown in Figs 3 and 6, and the envelope electric field $|\mathbf{E}|^2 = E_r^2 + E_\varphi^2 + E_z^2$ is given in Figs 4 and 7.

Quantities in Figs 1–7 are dimensionless. There are 64 points in the $r$-direction and 64 points in the $z$-direction in our numerical calculations. For the downward current region of the aurora, their relations with dimensional ones are (taking $T_e = 1 \times 10^5$ K, $n_e = 20$ cm$^{-3}$, $\alpha = 18\,800$, $\lambda_D = 5$ m) as follows [14]:

$$\begin{aligned}\phi &= 9(\phi)_{\text{Fig}}(V), \frac{|E|^2}{4\pi n_e T_e} = 7.23 \times 10^{-4}\,|E|^2_{\text{Fig}}, \\ z &= 3 \times 10^2 (z)_{\text{Fig}}(m), t = 1.09 \times 10^{-2}\tau(s).\end{aligned} \tag{3.7}$$

https://doi.org/10.1017/S0022377810000607 Published online by Cambridge University Press

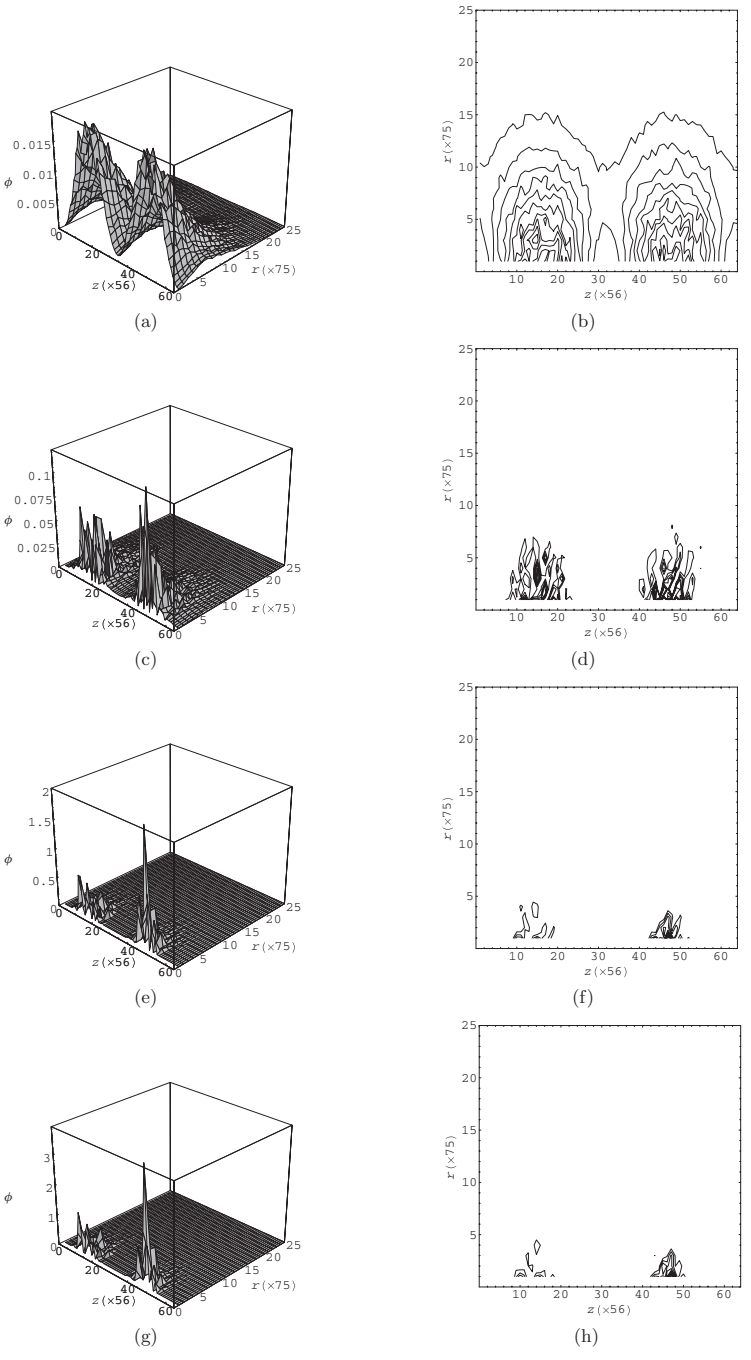


**Figure 2.** Collapse development and level contours of electric potential when $|E_{\max}|^2_{\tau=0} = 30$. (a) and (b) $\tau = 0.0018, \phi_{\max} = 2.06 \times 10^{-2}$, (c) and (d) $\tau = 0.144, \phi_{\max} = 0.12$, (e) and (f) $\tau = 0.2826, \phi_{\max} = 1.95$, (g) and (h) $\tau = 0.3195, \phi_{\max} = 3.80$.

https://doi.org/10.1017/S0022377810000607 Published online by Cambridge University Press

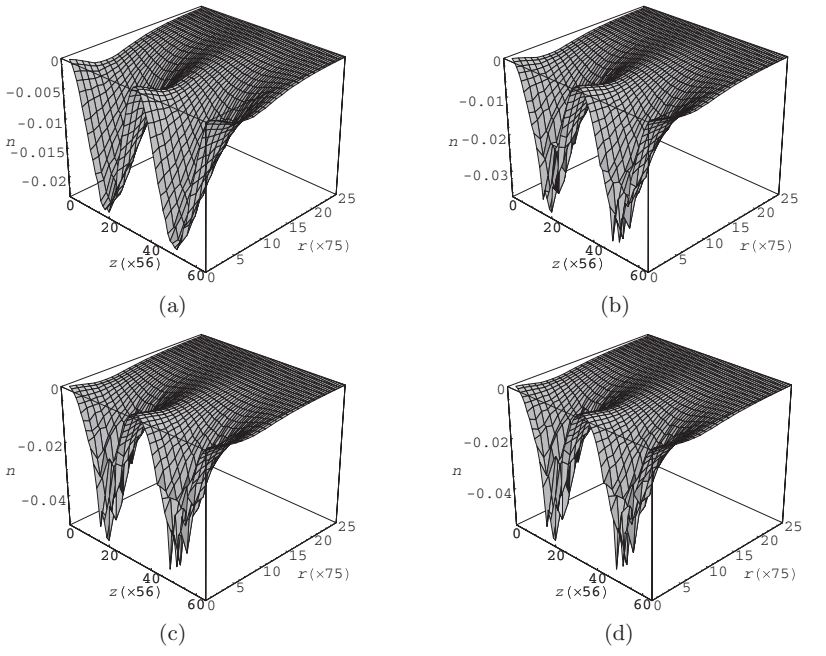


**Figure 3.** Collapse development of density disturbance when $|E_{\max}|^2_{\tau=0} = 30$. (a) $\tau = 0.0018$, $n_{\min} = -2.33 \times 10^{-2}$, (b) $\tau = 0.144, n_{\min} = -3.68 \times 10^{-2}$, (c) $\tau = 0.2826, n_{\min} = -5.09 \times 10^{-2}$, (d) $\tau = 0.3195, n_{\min} = -5.46 \times 10^{-2}$.

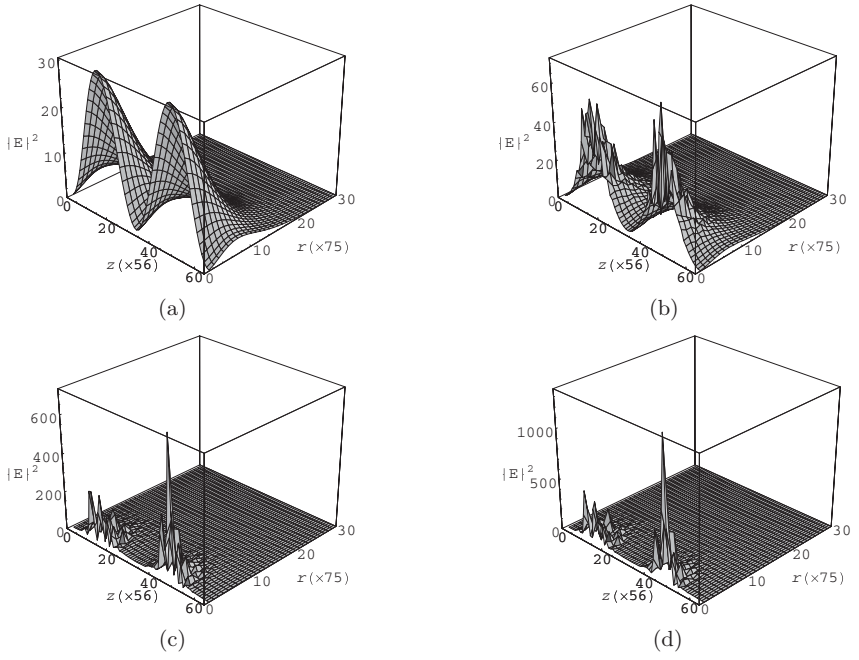


**Figure 4.** Collapse development of envelop electric field when $|E_{\max}|^2_{\tau=0} = 30$. (a) $\tau = 0.0018$, $|\mathbf{E}|^2_{\max} = 30.2$, (b) $\tau = 0.144, |\mathbf{E}|^2_{\max} = 72.8$, (c) $\tau = 0.2826, |\mathbf{E}|^2_{\max} = 705$, (d) $\tau = 0.3195, |\mathbf{E}|^2_{\max} = 1356$.

https://doi.org/10.1017/S0022377810000607 Published online by Cambridge University Press

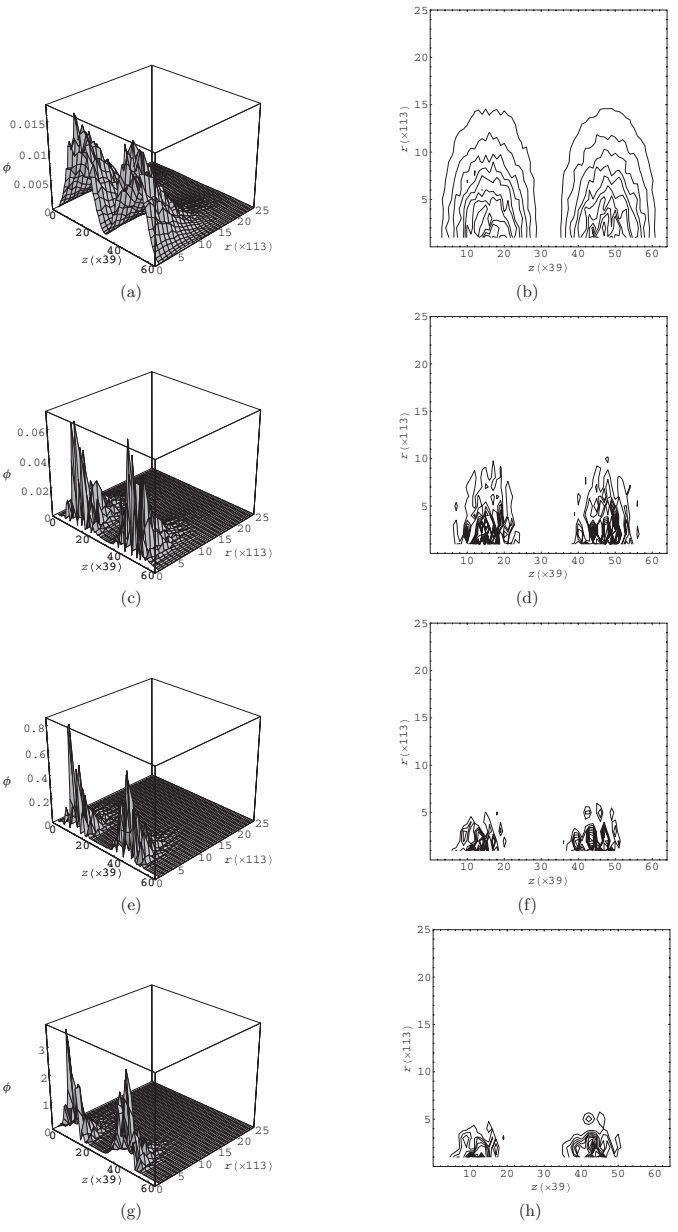


**Figure 5.** Collapse development and level contours of electric potential when $|E_{\max}|^2_{\tau=0} = 25$. (a) and (b) $\tau = 0.0018, \phi_{\max} = 1.79 \times 10^{-2}$, (c) and (d) $\tau = 0.1314, \phi_{\max} = 6.72 \times 10^{-2}$, (e) and (f) $\tau = 0.2358, \phi_{\max} = 0.83$, (g) and (h) $\tau = 0.2898, \phi_{\max} = 4.00$.

In Figs 2–4, we initially take $|E_{\max}|^2_{\tau=0} = 30$, the period and width are chosen as $z_0 = 3600$ and $r_0 = 600$. Figure 2 gives the ramp potential and width of the ramp as $\phi_{\max} = 3.80$ and $z = 1.0$, when $\tau = 0.3195$, using (3.7) to yield $\phi_{\max} = 34.2$ V, $z = 300$ m and the double layer becomes a double–double layer, so that the thickness of double layer's either side, $d = 150$ m $= 30\lambda_D$.

https://doi.org/10.1017/S0022377810000607 Published online by Cambridge University Press

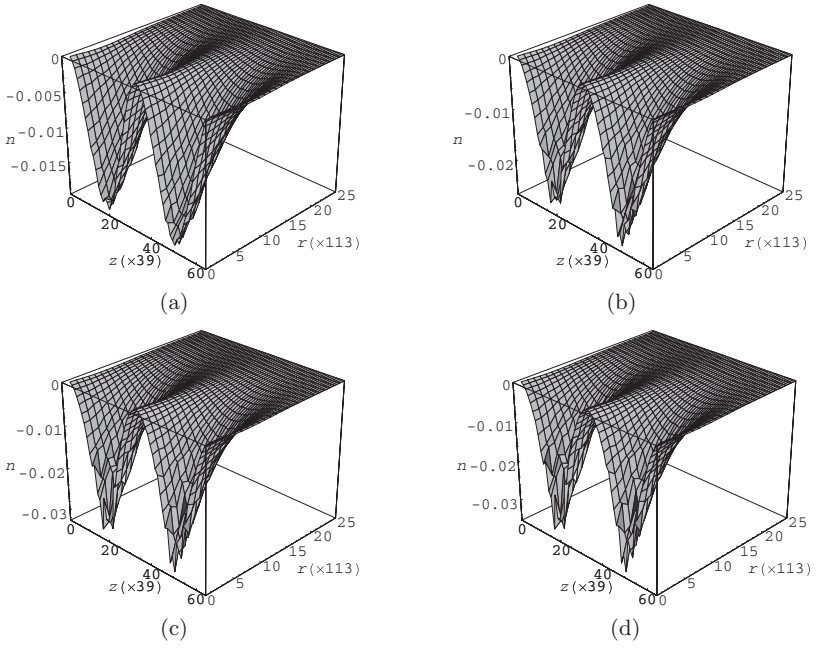


**Figure 6.** Collapse development of density disturbance when $|E_{\max}|^2_{\tau=0} = 25$. (a) $\tau = 0.0018$, $n_{\min} = -1.93 \times 10^{-2}$, (b) $\tau = 0.1314, n_{\min} = -2.66 \times 10^{-2}$, (c) $\tau = 0.2358, n_{\min} = -3.25 \times 10^{-2}$, (d) $\tau = 0.2898, n_{\min} = -3.56 \times 10^{-2}$.

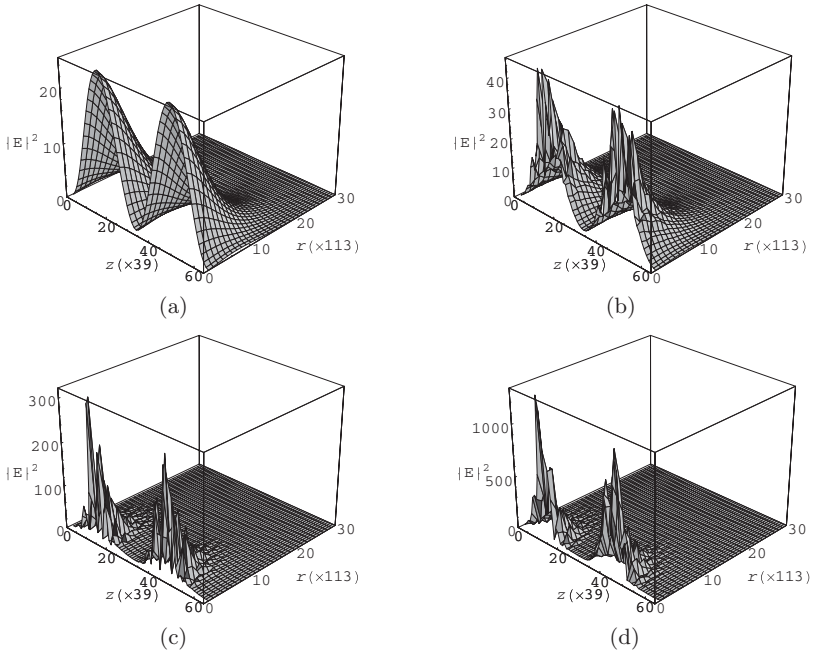


**Figure 7.** Collapse development of envelop electric field when $|E_{\max}|^2_{\tau=0} = 25$. (a) $\tau = 0.0018$, $|\mathbf{E}|^2_{\max} = 25.1$, (b) $\tau = 0.1314, |\mathbf{E}|^2_{\max} = 45$, (c) $\tau = 0.2358, |\mathbf{E}|^2_{\max} = 311$, (d) $\tau = 0.2898, |\mathbf{E}|^2_{\max} = 1399$.

https://doi.org/10.1017/S0022377810000607 Published online by Cambridge University Press

In Figs 5–7, we initially take $|E_{\max}|^2_{\tau=0} = 25$, $z_0 = 2500$ and $r_0 = 900$; Fig. 5 gives the ramp potential and width of the ramp as $\phi_{\max} = 4.00$ and $z = 0.8$, when $\tau = 0.2898$, i.e. $\phi_{\max} = 36.0$ V and $z = 240$ m so that the thickness of double layer's either side, $d = 120$ m $= 24\lambda_D$.

It is worth noting that the observations [14–15] by the FAST satellite in the downward current region of the aurora reveal that the ramp potential of the double layer is 14–40 V and the thickness of the structure is between 100 and 200 m, roughly tens of $\lambda_D$, which are similar to our results.

## 4. Conclusion and discussion

From the above study, we arrive at the following conclusions:

(1) From Figs 4 and 7, we can see that as time progresses, the initial electric field narrows and becomes more intense, i.e. it collapses. The corresponding density cavity also deepens and narrows as the ponderomotive force becomes stronger, as shown schematically in Figs 3 and 6. It is shown that at supersonic collapse the growth of the density lags behind the growth of the high-frequency field energy, which agrees with the theoretical predictions [25] and numerical results [23].

(2) From (2.10)–(2.12), localized drop in density owing to collapsed high-frequency field can lead to the formation of double–double layer. Li [16] proposed that double layer in the plasma, which is controlled by modulational instability, is a nonlinear entity in this case: soliton and wave-packet shock are one-dimensional. It is well know that the combined multidimensional entity, consisting of a nonlinear collapsing wave packet and its associated density well can be called a caviton [26]. Therefore, double layer is a nonlinear structure: caviton in two dimensions with three field components, which is similar to our results. From Figs 2 and 5, we can see that numerical results coincide well with the measurements in both the maximum peak potential and the thickness of the double layer by the FAST satellite in the downward current region, and there are a series of small potential ramps besides the maximum peak potential. That is to say, there exists two or more double layers in the downward current region of the aurora. These are consistent with Block's analysis [13].

(3) We have examined the problem of the linear instabilities for (2.10) and (2.11) in [23]. It has been shown analytically that the electric fields are modulationally unstable, and such instabilities would localize the electric fields. In this paper, we choose 64 points in the $r$-direction and $z$-direction. However, we would get the same results when increasing the number of grid points in the simulation. That is to say, such instability is not a numerical instability but a physical instability.

(4) The initial field condition (3.6) is not the only choice. The amplitude of any propagating transverse wave that is slowly varying function of time can be chosen as the initial condition if it satisfies the condition for a transverse wave. Different initial condition can lead to different detail collapse process, but the same collapse trend. In addition, it should be noted that the collapse tendency of electric potential is about the same for two different initial values, although the resulting potential ramp and thickness of double layers have slight difference in detail. This is a better result, which is not sensitive to the initial values. On the other hand, the results of numerical analysis have shown that when $|E_{\max}|^2_{\tau=0}$ increases and $r_0$ remains

https://doi.org/10.1017/S0022377810000607 Published online by Cambridge University Press

unchanged, the collapse for the field becomes fast; when $r_0$ increases and $|E_{\max}|^2_{\tau=0}$ remains unchanged, the collapse for the field becomes slow.

(5) When the time scales $\tau > 0.3195$ (see Fig. 4) and $\tau > 0.2898$ (see Fig. 7), the field collapses rapidly and leads to a strengthened field, then $\hat{W} = \frac{|\mathbf{E}(\mathbf{r},t)|^2}{8\pi n_0 T_e} = \frac{8}{3}\mu|\hat{\mathbf{E}}(\hat{\mathbf{r}},\tau)|^2 > 1$, and in this case stronger turbulent interactions occur between the field and the particles. The field energy will be transferred to the particles through these interactions. As the particle energy increases and the field energy decreases, $\hat{W}$ will decrease until the condition $\hat{W} < 1$ is satisfied again [26–27].

*Acknowledgements*

Sanqiu Liu is supported in this work by the National Natural Science Foundation of China under the grant No. 10963002, International S&T Cooperation Program of China (2009DFA02320) and Jiangxi Province Program for Innovative Research Team in Jiangxi Province and Nanchang University.

## References

[1] Alfvén, H. and Carlqvist, P. 1967 Currents in the solar atmosphere and a theory of solar flares. *Solar Phys.* **1**, 220.

[2] Evans, D. S. 1974 Precipitating electron fluxes formed by a magnetic field-aligned potential difference. *J. Geophys. Res.* **79**, 2853.

[3] Wescott, E. M., Stenbaek-Nielsen, M. C., Hallinan, T. J. and Davis, T. N. 1976 The skylab barium injection experiments: evidence for a double layer. *J. Geophys. Res.* **81**, 4495.

[4] Shawhan, S. D., Falthammar, C. G. and Block, L. P. 1978 On the nature of large auroral zone electric fields at 1 RE altitude. *J. Geophys. Res.* **83**, 1049.

[5] Leung, P. A., Wong, Y. and Quon, B. H. 1980 *Phys. Fluids* **23**, 992.

[6] Quon, B. H. and Wong, A. Y. 1976 Formation of potential double layers in plasmas. *Phys. Rev. Lett.* **37**, 1393.

[7] Coakley, P. and Hershkowitz, N. 1979 Laboratory double layers. *Phys. Fluids* **22**, 1171.

[8] Knorr, G. and Goertz, C. K. 1974 Existence and stability of strong potential double layers. *Astrophys. Space Sci.* **31**, 209.

[9] Hudson, M. K., Lottko, W., Roth, I. and Witt, E. 1983 Solitary waves and double layers on auroral field lines. *J. Geophys. Res.* **88**, 916.

[10] Izuka, S., Saeki, K., Sato, N. and Hatta, Y. 1979 Buneman instability, pierce instability, and double-layer formation in a collisionless plasma. *Phys. Rev. Lett.* **43**, 1404.

[11] Torven, S. 1981 Modified Korteweg-de Vries equation for propagating double layers in plasma. *Phys. Rev. Lett.* **47**, 1053.

[12] Block, L. P. 1972 Potential double layers in the ionosphere (ionospheric double layer theory extended to conditions, including gravity and expansion effects in diverging geomagnetic flux tubes). *Cosm. Electrodyn.* **3**, 349.

[13] Block, L. P. 1978 A double layer review. *Astrophys. Space Sci.* **55**, 59.

[14] Ergun, R. E., Su, Y. -J., Andersson, L., Carlson, C. W., McFadden, J. P., Mozer, F. S., Newman, D. L., Goldman, M. V. and Strangeway, R. J. 2001 Direct observation of localized parallel electric fields in a space plasma. *Phys. Rev. Lett.* **87**, 045003.

[15] Ergun, R. E., Andersson, L., Carlson, C. W., Newman, D. L. and Goldman, M. V. 2003 Double layers in the downward current region of the aurora. *Nonlinear Process. Geophys.* **10**, 45–52.

[16] Li, X. Q. 1985 Double layers in strong turbulent plasmas. *Astrophys. Space Sci.* **112**, 13.

[17] Newman, D. L., Goldman, M. V., Ergun, R. E. and Mangeney, A. 2001 Formation of double layers and electron holes in a current-driven space plasma. *Phys. Rev. Lett*. **87**, 255001.

[18] Raadu, M. A. and Carlqvist, P. 1981 Electrostatic double layers and a plasma evacuation process. *Astrophys. Space Sci*. **74**, 189.

[19] Carlqvist P. 1980 Studies of electrostatic double layers with applications to cosmic plasmas. In: *Electron and Plasma Physics*. Stockholm, Sweden: Royal Institute of Technology, TRITA-EPP-80.

[20] Thornhill, S. G. and ter Haar, D. 1978 Langmuir turbulence and modulational instability. *Phys. Rep*. **43C**(2), 43.

[21] Nicholson, D. R. and Goldman, M. V. 1978 Cascade and collapse of Langmuir waves in two dimensions. *Phys. Fluids* **21**, 1766.

[22] Zakharov, V. E. 1983 Nonlinear phenomena and plasma turbulence. In: *Handbook of Plasma Physics*, Vol. 2 (ed. A. A. Galeev and R. N. Sudan). Amsterdan, Netherlands: North-Holland, pp. 81–122.

[23] Liu, X. L. and Liu, S. Q. 2006 Numerical analysis of strong Langmuir turbulence excited by transverse plasmons in a laser plasma. *J. Plasma Phys*. **73**, 3.

[24] Robinson, P. A. 1997 Nonlinear wave collapse and strong turbulence. *Rev. Mod. Phys*. **69**, 507.

[25] Rubenchik, A. M. and Zakharov, V. E. 1991 *Handbook of Plasma Physics*, Vol. 3 (eds. M. N. Rosenbluth, R. Z. Sagdeev, A. M. Rubenchik and S. Witkowski). Amsterdam, Netherlands: North-Holland, p. 335.

[26] Li, X. Q. 2004 *Collapsing Dynamics of Plasmons* (in Chinese). Beijing, China: Chinese Science and Technology Press, pp. 126–148.

[27] Tsytovich, V. N. 1977 *Theory of Turbulent Plasma*. New York, NY: Consultants Bureau, p. 44.